JOURNAL OF GEOPHYSICAL RESEARCH, VOL. 105, NO. A10, PAGES 23,323–23,338, OCTOBER 1, 2000

CRRES observations of density cavities inside the plasmasphere

D. L. Carpenter,[1] R. R. Anderson,[2] W. Calvert,[3] and M. B. Moldwin[4]

Abstract. Deep density troughs inside the plasmasphere in which electron density was a factor of from ~2 to 10 below nearby plasmasphere levels were found in ~13% of 1764 near-equatorial electron density profiles derived from the sweep frequency receiver data acquired in 1990-1991 by the CRRES satellite. These "inner troughs" appeared in the aftermath of plasmasphere erosion episodes and are interpreted as the near-equatorial manifestations of geomagnetic-field-aligned cavities. Inner troughs were found at all local times but were most common in the 1800-2400 magnetic local time (MLT) sector and least common between 0600 and 1200 MLT. Their inner boundaries, plasmapause-like in form, were mostly at $L < 3.5$ but in ~30% of the cases were at $L < 2.5$ under geomagnetic conditions that traditionally have been associated with plasmapause radii in the L = 3-3.5 range or beyond. The trough outer walls were exceptionally steep, in several cases exhibiting a factor of 4 or more density change within less than 100 km along the near-equatorial satellite orbit. The extent of the troughs in L ranged from $\Delta L \sim 0.5$ to 2, and various forms of evidence, including earlier studies, suggest an extent of more than 20° in longitude. Such evidence includes plasma waves propagating in a free space mode within the inner trough while extending in frequency well above the upper limit of trapped continuum radiation detected beyond the plasmasphere. We suggest, as have previous authors, that the troughs are translated vestiges of plasma configurations established during preceding periods of plasmasphere erosion. In some such cases, dense plasma features lying beyond the troughs were probably connected to the main plasmasphere in a local time sector to the east of the observing longitude. However, in some of the cases of troughs with steep outer walls the dense plasma feature beyond that wall may have been shaped by a mechanism for detaching plasma from an originally larger outer plasmasphere, such as by shear flows in the premidnight sector associated with subauroral ion drifts.

1. Introduction

1.1. The Plasmasphere: Known, Yet Unknown

Much is known about the plasmasphere, as is demonstrated by *Lemaire and Gringauz* [1998] in their recent monograph on the subject. Their work recalls the efforts made 30 years ago to describe certain main features of the plasmasphere and to interpret the available observations in terms of the interplay among (1) global-scale magnetospheric convection, (2) the electric field associated with the Earth's rotation, and (3) interchange fluxes that couple the ionosphere to overlying regions. This monograph covers many aspects of the present knowledge and interpretation of the plasmasphere, including changes in plasmaspheric morphology that occur in response to storms and substorms, the role of instabilities in the plasmasphere erosion process, plasmaspheric refilling through interchange fluxes, and the ion composition and thermal structure of the plasmasphere. There is also an extensive bibliography, to which the reader is referred.

This monograph brings together within a relatively coherent framework materials that have been widely dispersed in the literature while also pointing to broad gaps in our knowledge and understanding. These gaps should arouse interest among those in the community who may believe that the plasmasphere is already well known and well understood. One such gap involves the cycle of plasmaspheric erosion and recovery. Much has been learned about the shape of the plasmasphere and of the density replenishment process at various stages of a plasmasphere erosion/recovery cycle, for example, from measurements at geosynchronous orbit [e.g., *Moldwin et al.*, 1994; *Moldwin*, 1997]. Theoretical models of plasmaspheric dynamics have also had some success in explaining reported observations [e.g., *Weiss et al.*, 1997; *Ober et al.*, 1997]. However, the plasmasphere exhibits a number of density features that until now have only been partially described and which are far from understood [e.g., *Carpenter and Lemaire*, 1997]. This paper concerns one such feature, a low-density region inside what appears to be the main body of the plasmasphere. This inner trough or "plasmaspheric cavity" appears to be fundamental to the way the cold plasma evolves in the aftermath of periods of enhanced convection. As such, it is relevant to as yet unanswered questions about the physical processes that control the geoelectric field at subauroral latitudes and about the physics involved in the establishment of a plasmapause boundary at a new location.

1.2. Previous Observations

1.2.1. Illustration. Figure 1 shows how the plasmaspheric cavity effect is manifested in a near-equatorial electron density profile obtained from the sweep frequency receiver (SFR) data on ISEE 1 [*Gurnett et al.*, 1979] along an inbound orbit in the dusk sector. The density rose steeply at $L \sim 4.2$ to plasmasphere levels from values typical of the "main plasma trough," or "magnetospheric cavity," as it is often called. Then at $L \sim 3.5$ a steep outer wall of another trough was encountered. Within this inner trough the density was a factor of ~5 below nearby plasmaspheric levels. A relatively steep interior wall of the trough was detected at $L \sim 2.8$ as the density returned to plasmaspheric levels and the end of the data stream was reached.

1.2.2. Early work on trough effects. Several forms of density depression separating regions of cold, dense plasma have been de-

[1] Space, Telecommunications, and Radioscience Laboratory, Stanford University, Stanford, California.
[2] Department of Physics and Astronomy, University of Iowa, Iowa City.
[3] Iowa City, Iowa.
[4] Department of Physics and Space Science, Florida Institute of Technology, Melbourne.

Paper number 2000JA000013.
0148-0227/00/2000JA000013$09.00

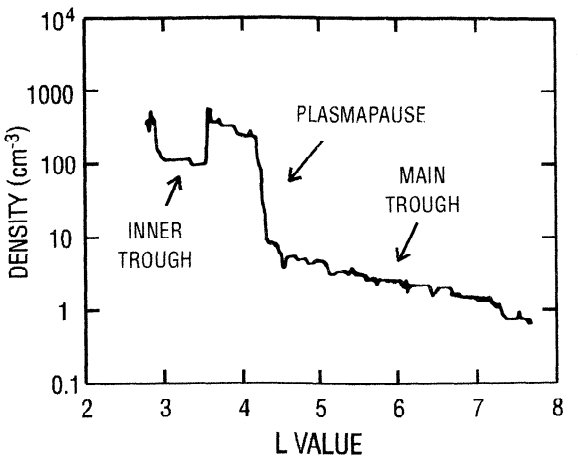

Figure 1. A near-equatorial electron density profile from ISEE 1 showing an example of a plasmaspheric cavity in the dusk sector at 1900 -1700 MLT on September 17, 1983. The electron density was derived from the sweep frequency receiver (SFR) records of plasma wave emissions as described for CRRES in section 2.1 (adapted from *Carpenter and Anderson* [1992]).

scribed previously. In the early 1970 s, *Chappell et al.* [1971] employed an ion mass spectrometer on OGO 5 to study the near-equatorial ion density distribution in the magnetosphere. They reported finding regions of dense plasma of the order of 1 R_E in extent beyond the main plasmasphere in the outer afternoon-dusk sector. It was inferred that these outlying dense plasma features or outliers had been detached from the main plasmasphere during preceding periods of enhanced convection activity [e.g., *Chappell,* 1974].

Early indications of plasmaspheric trough effects within the plasmasphere were also reported by *Carpenter* [1970], who found from whistlers that within the duskside plasmasphere bulge region, the density profile out to a distance corresponding to that of the afternoon (prebulge) plasmapause was frequently not joined smoothly to the plasmaspheric-level segment beyond. In some cases the transition was marked by a trough-like depression by a factor of ~2 in density. Further evidence of trough-like features within the plasmasphere was provided by *Taylor et al.* [1971, p. 6806] from an ion mass spectrometer on the polar orbiting satellite OGO 4. Drawing upon earlier evidence of a link between light ion troughs in the ionosphere and the plasmapause [e.g., *Taylor et al.,* 1969; *Carpenter et al.,* 1969; *Grebowsky et al.,* 1970; *Mayr et al.,* 1970], the authors described a sequence of latitudinal profiles at ~900 km altitude that exhibited

> "a pronounced inner trough, in which the ambient H+ concentrations decrease by an order of magnitude near L = 2 and subsequently recover to midlatitude concentration levels before a more pronounced and persistent trough is encountered at higher L positions. The time evolution of the trough boundaries observed during a sample of five consecutive satellite orbits following the peak of the magnetic storm on September 21, 1967, suggests that the observed structure results from a plasma tail or elongation of the plasmasphere that tends to corotate with the Earth."

Later, from whistler data acquired in Antarctica in 1965 and 1966, *Ho and Carpenter* [1976] reported on three cases of plasmaspheric density troughs that were detected for periods of 12 hours or more under conditions of quieting following moderate magnetic disturbance. These observations employed a scanning process involving relative east-west motion, at about one-tenth of the Earth's angular velocity or greater, between density features and the observing whistler station or stations. These authors [*Ho and Carpenter,* 1976] reported "outlying high density regions at ~ 4- 6 R_E that are separated from the main plasmasphere by trough-like depressions ranging in width from ~0.2 to 1 R_E." They suggested that "at least a major class of the density structures that develop near 4 R_E are tail-like in nature, joined to the main body of the plasmasphere."

A key finding was reported in 1990 by *Horwitz et al.* [1990], who presented results of a statistical study of plasmasphere structure from the retarding ion mass spectrometer (RIMS) on DE 1. Their density profile categories included a class of ion density troughs of the order of $\Delta L = 0.5$ in width that were apparently embedded in the plasmasphere, typically at $L < 3$. Such profiles were found to occur predominantly in the dusk sector, on roughly 10% of the orbits studied. Profiles similar to those reported by Horwitz et al. had also been encountered in surveys of the large body of ISEE SFR data on near-equatorial electron density, as illustrated in Figure 1.

An apparently related phenomenon was also reported by *Oya* [1991], who studied electron density profiles from an SFR on EXOS D (Akebono), which was in a 75° inclination orbit with and apogee of ~10,000 km. On some orbits during periods of recovery from disturbance, depressed densities were found near the equator at $L \sim 2.5$. When apogee was near the equator, the corresponding electron density-versus-time profiles exhibited conjugate density peaks at off-equatorial latitudes, indicating a belt of higher-density plasma beyond $L = 2.5$. The off-equatorial peaks were described as "donkey ears."

The SFR data from the CRRES satellite provides a unique opportunity for an in-depth description of plasmaspheric cavity phenomenon. In the following, a variety of well-defined trough events are illustrated, and attention is called to features such as the steepness of the outer cavity walls and the occasional location of their plasmapause-like inner walls at $L < 2.5$ under geomagnetic conditions for which a plasmapause at $L < 2.5$ would not be expected. In section 2.3 we will also discuss the presence of plasma wave emissions within and near plasmaspheric cavities, and in section 2.4.5 we will use these emission data to draw inferences concerning the spatial extent of the cavities. The main observed features of the troughs are then summarized. Finally, we discuss ways in which the cavities appear to challenge the conventional wisdom about the behavior of the plasmasphere.

2. Observations

2.1. CRRES Measurements

The CRRES data were acquired over a 14 month period in 1990-1991 along near-equatorial orbits with a perigee altitude of 350 km and an apogee at 6.3 R_E geocentric distance. The SFR sampling interval, which was 8 s for the frequency bands 6.4-50 kHz and 50- 400 kHz, 16 s for 0.8 - 6.4 kHz, and 32 s for 0.1- 0.8 kHz [*Anderson et al.,* 1992], provided spatial resolution in electron density measurements of the order of 50 km at typical plasmapause distances, a factor of 4 improvement over that achievable from the ISEE SFR (32 s in all bands). The CRRES orbital period of about 10 hour also made it possible to identify certain important changes in the plasmasphere that can take place in response to multihour periods of substorm activity.

Figure 2a provides an example of the SFR data format for a full 10-hour orbit. Electric field emissions from 1-400 kHz are plotted versus time as CRRES moved outward through the plasmasphere to an apogee at $L \sim 7.3$ and back during orbit 145 on September 23, 1990. In Figure 2b is a corresponding plot of the electron density versus time that was derived from the upper hybrid resonance

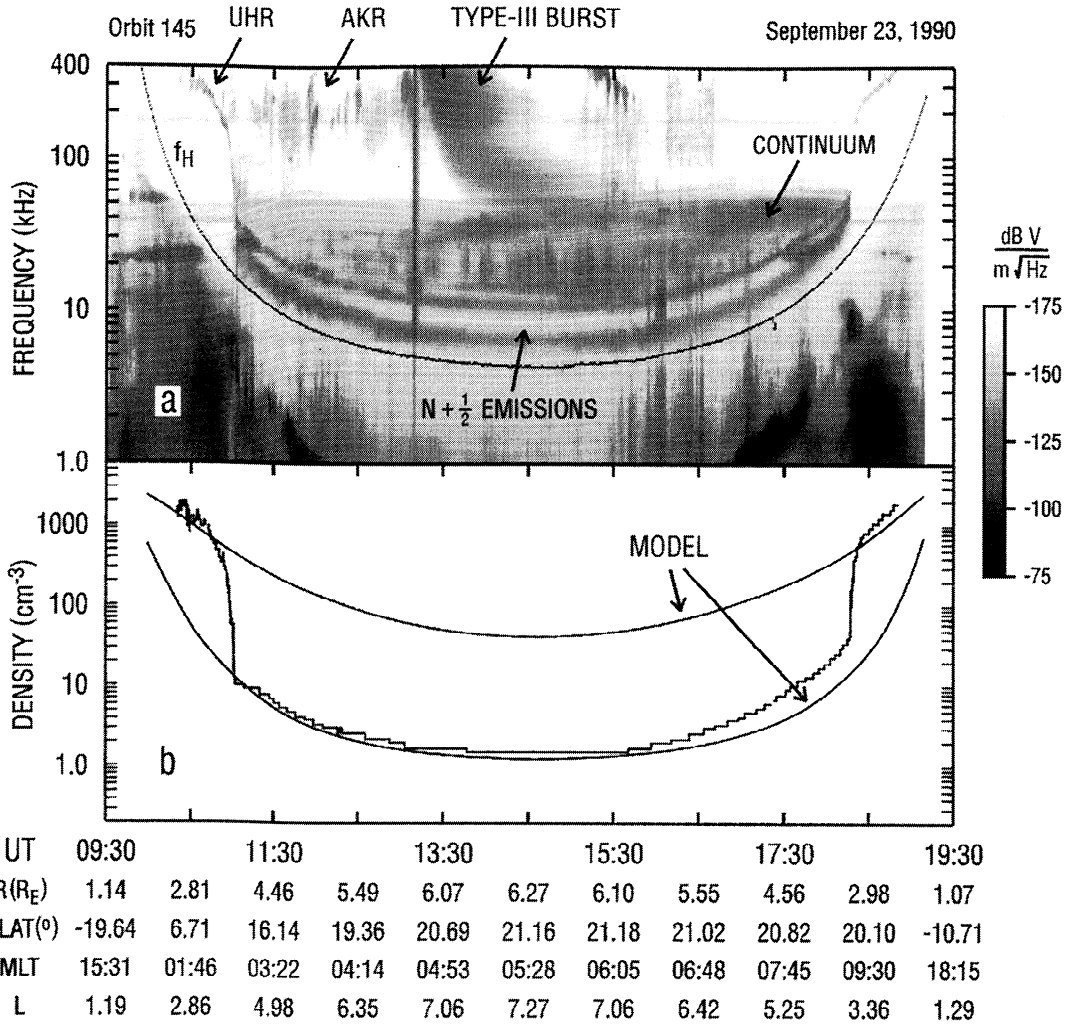

Figure 2. Sweep frequency receiver data from CRRES showing an unusually simple configuration of the plasmasphere and main plasma trough. (a) A 10 hour grayscale record displaying wave activity from 1 to 400 kHz versus time along orbit 145 on September 23, 1990. Arrows and labels identify several of the wave emissions commonly encountered by CRRES. The value of the local electron gyrofrequency along the orbit is marked f_H. (b) Corresponding plot of electron density versus time derived from variations with time in the upper hybrid resonance (UHR) emission band and the plasma frequency cutoff. The model curves are from empirical equatorial density models developed by *Carpenter and Anderson* [1992], where the upper curve represents quiet plasmaspheric conditions and the lower curve represents the nightside main plasma trough.

(UHR) emissions [*Gurnett et al.*, 1979] or the plasma frequency cutoff [*Gurnett and Shaw*, 1973]. Also note in Figure 2a and on later SFR records that there is often a sudden change in the spectral density at 50 kHz. At this frequency the receiver bandwidth changed from 400 Hz in the band from 6.4 - 50 kHz to 3.2 kHz in the band from 50 - 400 kHz. The channel gains for these bands were set so a strong monochromatic signal would appear continuous across the band boundary. Because of the increase in bandwidth, a weak diffuse signal near the noise level will therefore often appear to become artificially weaker at this frequency.

Within the plasmasphere the UHR emissions are usually well defined, as shown on the left in Figure 2a, appearing as a narrow band separating a quiet part of the spectrum immediately below from a higher-frequency region that is often populated by type-III solar bursts or auroral kilometric radiation (AKR). Beyond the plasmasphere, in the main plasma trough region, the UHR is usually not well defined. The electron density is then determined from the lower limiting frequency of continuum radiation, which is interpreted as a plasma wave cutoff at the plasma frequency [*Gurnett and Shaw*, 1973]. The experimental error that is associated with measuring the UHR or plasma frequencies on the SFR records is estimated to be ±6%, which corresponds to ±12% in density. Note that the 400 kHz upper limit of the SFR data imposes an upper limit of ~2000 el cm^{-3} on the electron density that can be measured by this method.

Figure 3 puts the density profile of Figure 2b into spatial perspective by plotting the log of the electron density vertically with respect to a plane that is defined by satellite L value as a function of magnetic local time. The viewpoint is at an elevation angle 60° above the L-MLT plane and along the midnight meridian. Because of the satellite's low magnetic latitude (usually < 30°), the radial coordinate is a rough measure of geocentric distance. In both Figures 2b and 3 the model curves are from ISEE-based empirical models of *Carpenter and Anderson* [1992]. The upper curve

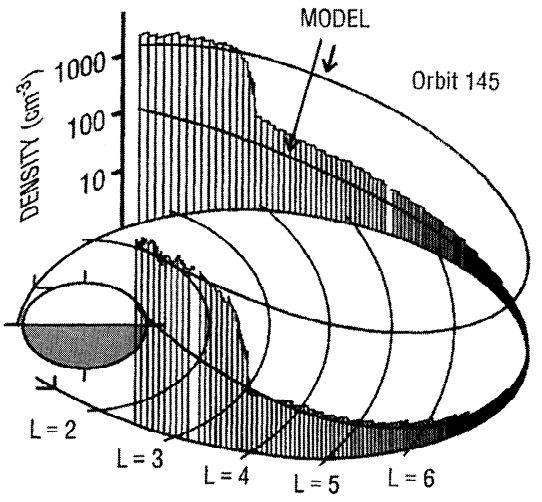

Figure 3. A plot in cylindrical coordinates of the data of Figure 2b in which the logarithmic electron density is shown vertically as a function of L value and magnetic local time along orbit 145. The viewpoint is from the midnight meridian at an elevation angle of 60° above the L-MLT plane.

represents quiet time conditions within the plasmasphere and the lower curve represents nighttime (~0200 MLT) conditions in the low-density main plasma trough region.

On the SFR records the distribution of plasma wave phenomena offers insight into plasma density structure, since certain classes of waves tend to be excluded from, or confined within, particular features of the plasma. On the record of Figure 2a are marked a number of emissions typically observed in the CRRES data, among them a type-III solar burst, bursts of auroral kilometric radiation (AKR), continuum radiation, and n + ½ electron cyclotron harmonic (ECH) radiation. The n + ½ ECH bands are usually confined to the main plasma trough region outside the plasmasphere. The manner in which they track the local gyrofrequency f_H, as indicated by the thin dark curve in Figure 2a, implies that they are electrostatic in nature [e.g., *Kennel et al.*, 1970; *Shaw and Gurnett*, 1975; *Hubbard and Birmingham*, 1978; *Ashour-Abdalla et al.*, 1979; *Paranicas et al.*, 1992]. In contrast, the continuum radiation, also confined to the low density region in this case, is often found to extend upward from a lower limit that is inferred to be the local plasma frequency [*Gurnett and Shaw*, 1973]. When interpreted as "trapped continuum" it is believed to represent a free space electromagnetic mode propagating back and forth between the plasmapause and magnetopause but limited in frequency to the maximum plasma frequency in the magnetosheath [*Gurnett and Shaw*, 1973; *Kurth et al.*, 1981].

2.2. Plasmaspheric Troughs

2.2.1. Orbits 145 and 146: Structure during quieting. Density profiles as simple as those shown in Figures 2b and 3 are not common, appearing on only about 10% of the CRRES orbits for which SFR records are available. Outbound in the post midnight sector (see Figure 3), the density followed quiet plasmaspheric levels and then at $L \sim 4$ fell off relatively steeply by a factor of 20. In the main plasma trough region the profile smoothly followed the nighttime model, reaching a density minimum of ~1 el cm^{-3} near local dawn. In the morning sector the effects of dayside refilling were apparent, since the main trough density rose steadily with increasing local time in proportion to the nighttime model level. Then, at $L \sim 3.8$ inbound, a steep plasmapause was again encountered and the profile rose to near the quiet time plasmaspheric levels.

A much different density configuration was observed on the next orbit, illustrated using a similar format in Figures 4 and 5. Magnetic conditions had been calm during the orbit of Figure 2 ($Kp \sim 2+$). The following hours were still quieter, and one might have expected some redistribution into the postmidnight and dawn sectors of outlying dense plasma previously accumulated in the afternoon and dusk sectors. Indeed, dense, highly structured plasma now extended well beyond the plasmapause L values found on the previous orbit, and density troughs with well defined outer walls appeared both inbound and outbound within the L = 3-4 range.

Outbound in the post midnight sector (Figure 5), the density fluctuated rapidly by ~50% over spatial scales of order 100 km. Then at $L \sim 3$ the density dropped by a factor of ~5 into a narrow trough-like region. Larger, factor of 2-3 irregularities with scale lengths ~200-300 km appeared in the region of steep negative density gradients and just beyond in the trough proper. At $L \sim 3.7$, at the outer edge of the trough, the density returned abruptly to comparatively high plasmasphere values and then fell gradually but steadily out to $L \sim 4.7$, where it dropped sharply toward the nighttime main trough model level. Near apogee the density varied smoothly at a level close to that of the previous orbit (compare Figures 2b and 4b). Then, inbound near L = 6 in the morning sector, CRRES encountered several isolated irregularities with density enhancement factors of 2 to 4 and with spatial extent in the range 500-1000 km (see Figure 4). A plasmapause-like boundary was crossed at $L \sim 5.5$ and was followed by a profile that roughly mirrored the outbound distribution. A dense but irregular region was followed by an inner trough between $L \sim 4$ and ~ 3.6 and then irregularities in which the peak density rose to quiet plasmasphere levels near L = 3. Note in Figures 4b and 5 that while the densities near L = 6 were near the nighttime main trough model, the densities inside the inner troughs were nearly a factor of 3 above the model level at similar L values.

Figures 3 and 5 show how quickly the plasmaspheric configuration in a particular local time sector can change and that the change can include the appearance of interior cavities. Some of the differences between orbits might then be attributed to changes in convection in which a complex structure that is established at an earlier local time rotates into the local view of CRESS. In sections 2.2.2-2.2.4 we show additional evidence of plasmaspheric cavities, with emphasis on well-defined cases at $L < 3$.

2.2.2. Orbit 813 and 808 through 815. Figure 6 shows the SFR record and associated density-versus-time plot for orbit 813, on which apogee was at ~1800 MLT, ~12 hours from the time of apogee in Figure 5. In the density profile in Figure 6b there appear to be two troughs, at the left a broad one leading to an outlier at $L \sim 5.5$ and at the right a much narrower one. The situation is clarified by the corresponding plot of density versus satellite position, shown in Figure 7f as part of the orbital sequence 808 through 815. Outbound in the early afternoon sector the plasmapause was crossed at $L \sim 2.3$, and the densities were then characteristic of the dayside main trough [e.g., *Carpenter and Anderson*, 1992] until an outlier was reached. The outlier appeared in the local time sector ~1500-1600 MLT, where crossings of extensions of the plasmasphere by geosynchronous satellites are relatively common [e.g., *Higel and Wu*, 1984; *Moldwin et al.*, 1994; *Gallagher et al.*, 1995]. In fact, the plasma analyzer on geosynchronous satellite 1989-046 passed through a localized region of patchy, dense plasma between 1500 and 1700 MLT at approximately the time of this outlier encounter by CRRES. Later, along the inbound CRRES orbit at local

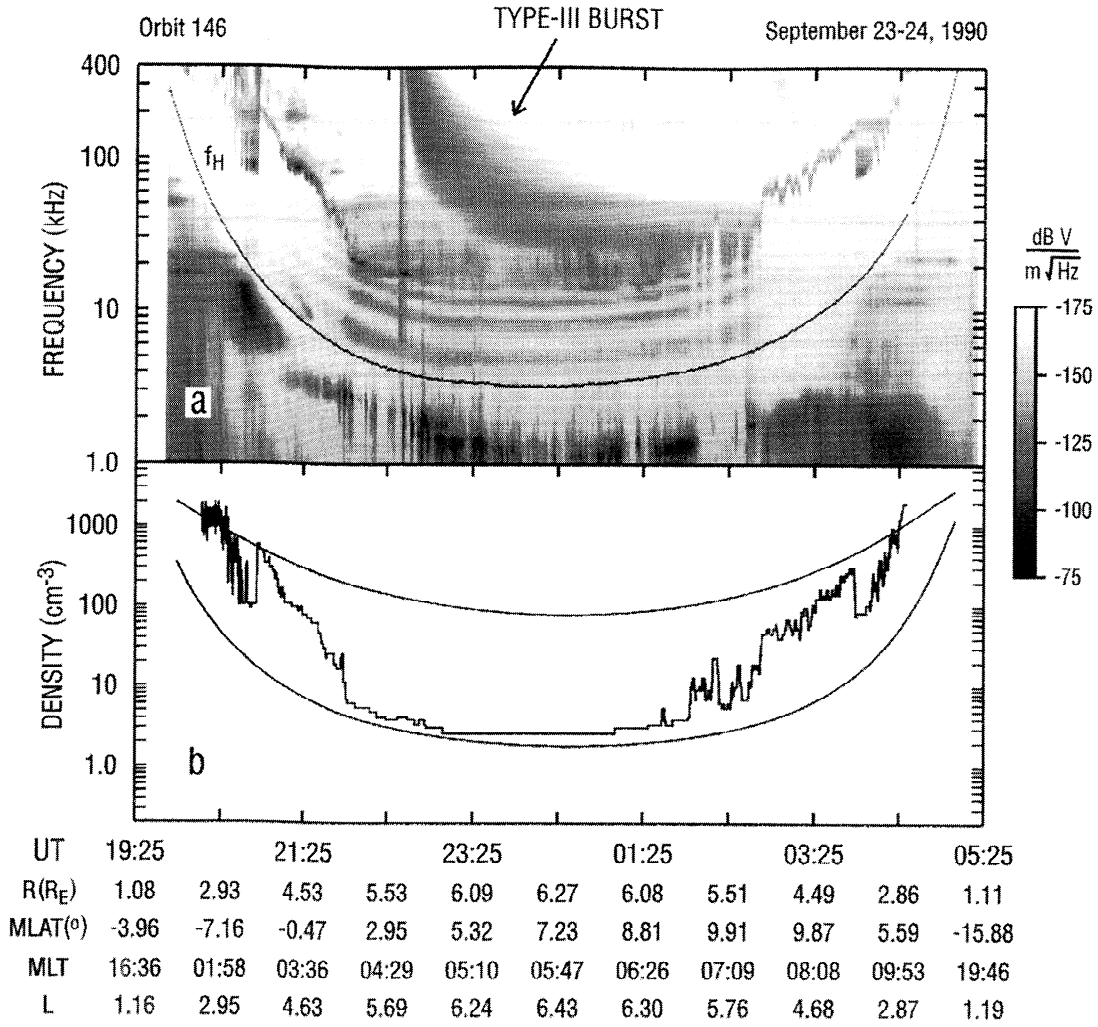

Figure 4. (a) SFR record for CRRES orbit 146, showing a plasma wave distribution substantially different from that observed only 10 hours earlier (Figure 2a). (b) Corresponding plot of electron density, showing highly structured plasma distributions that included narrow density troughs both inbound and outbound.

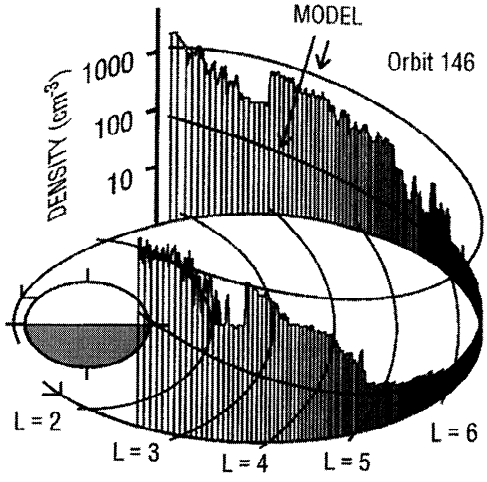

Figure 5. Perspective plot of the density data of Figure 4 b, showing by comparison to Figure 3 how quickly the plasma distribution in a given local time sector can change, even during calm geomagnetic conditions. Dense, structured plasma appeared well beyond the plasmaspheric limits along the preceding orbit.

times after dusk, the density moved lower, closer to the nighttime main trough model level (see also Figure 6 b). At $L \sim 4.2$, CRRES appeared to enter the plasmasphere but then encountered an inner trough with a steep outer boundary at $L \sim 3.3$ and a well-defined inner limit near $L = 2.3$. Within the trough the density varied smoothly at a level that was a factor of 5 below the quiettime model but still a factor of 2 or 3 above an inward projection of the trough model that is indicated for the main trough region beyond $L = 4$ (see Figure 6 b).

How does one distinguish the broad trough in the afternoon sector at the left in Figure 6b from the narrower one in the evening sector on the right? Both lie between a plasmapause-like density decrease and a dense outlier. As our later discussion suggests, the two may represent only slightly different stages in the plasmaspheric erosion and recovery cycle. However, for descriptive convenience we separated the two by requiring that the outer wall of an inner trough be at $L < \sim 4.5$. This usually meant that the inner limit of the trough was at $L < 3.5$. Thus, among the eight profiles in Figure 7, the afternoon (outbound) structures on orbits 810 and 811 (Figures 7c and 7d) may be somewhat arbitrarily classified as inner troughs. Our inner trough criteria also have a counterpart in terms of plasma temperature. On the SFR records a broad after-

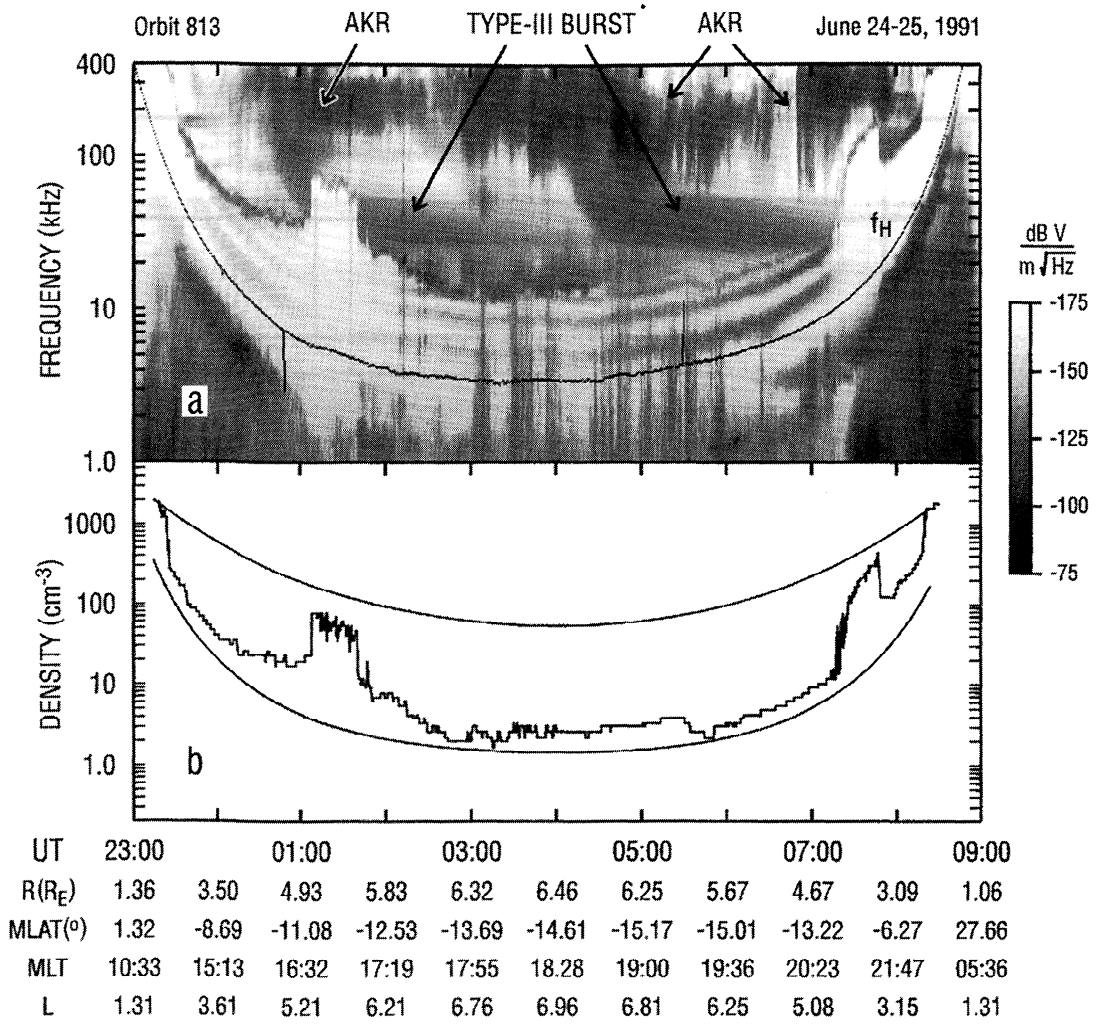

Figure 6. (a) SFR record from orbit 813, when the CRRES apogee was at ~1800 MLT. (b) Corresponding electron density plot, showing evidence of a well-defined plasmaspheric cavity at the right.

noon trough may show some indications of n + ½ ECH wave bands, as at the left in Figure 6a, whereas during crossings of most well-defined inner troughs, as at the right in Figure 6a and in both cases in Figure 4 a, such wave bands did not appear.

In the data of Figure 7 a well-defined inner trough in the dusk sector appeared on successive orbits 812 and 813 (Figures 7e and 7f), and a less well defined, shallower trough appeared on orbit 814. The density distributions on orbits 812 and 813 were remarkably similar except for a data gap on the inbound leg of orbit 812. As in Figure 5, these inner troughs appeared during a quieting trend in geomagnetic activity. The *AE* index for the period of Figure 7, from June 22 to June 26, 1991, is shown in Figure 8, with the 8 orbital periods in Figure 7 indicated below. There was a pronounced surge of the *AE* index on June 23 to peaks above 1000 and a subsequent quieting trend punctuated by brief surges to 600-700.

A notable feature of Figure 7 is the repeated appearance of an outlying high-density region in the afternoon sector. During and immediately following the surge in *AE* (orbits 809 - 811), this outlier appears to have broadened in extent along the orbit as its inner edge was displaced to lower L values. As quieting developed during and following orbit 812, the outlier became narrower in extent along the orbit and was displaced to higher L values. Corresponding outlier positions at geosynchronous orbit at various times during CRRES orbits 808, 811, 0813, and 814 were found in low-energy plasma analyzer data [e.g. *McComas et al.*, 1993] from the Los Alamos National Laboratory (LANL) satellite 1989-046. Overall, the afternoon outliers appear to have behaved as expected from previous measurements at geosynchronous orbit [e.g., *Elphic et al.*, 1996] as well as from convection modeling studies applied to periods of enhanced convection [e.g., *Weiss et al.*, 1997]. However, the same cannot be said for the evening sector troughs. Their detection after CRRES appeared to have reentered the plasmasphere, and their extent inward to $L \sim 2.3$, are further cause for reexamination of assumptions about the simplicity of the plasmaspheric system.

2.2.3. Orbit 1033: Trough during moderately high *Kp*. Another example of density cavity effects just beyond $L = 2$ and of highly structured plasmas in the dusk sector is shown in Figures 9 and 10. In this case, from orbit 1033 on September 27, 1991, the current geomagnetic activity was higher than in the examples described in section 2.2.2, with *Kp* in the range 5 to 5+ following a 48-hourr period of *Kp* values between 4+ and 6. Figures 9a and 9b show, respectively, the 10-hour SFR record and on an expanded scale the same data for the 2-hour period 1620-1820 UT, during which an inner trough was crossed. The disturbed geomagnetic

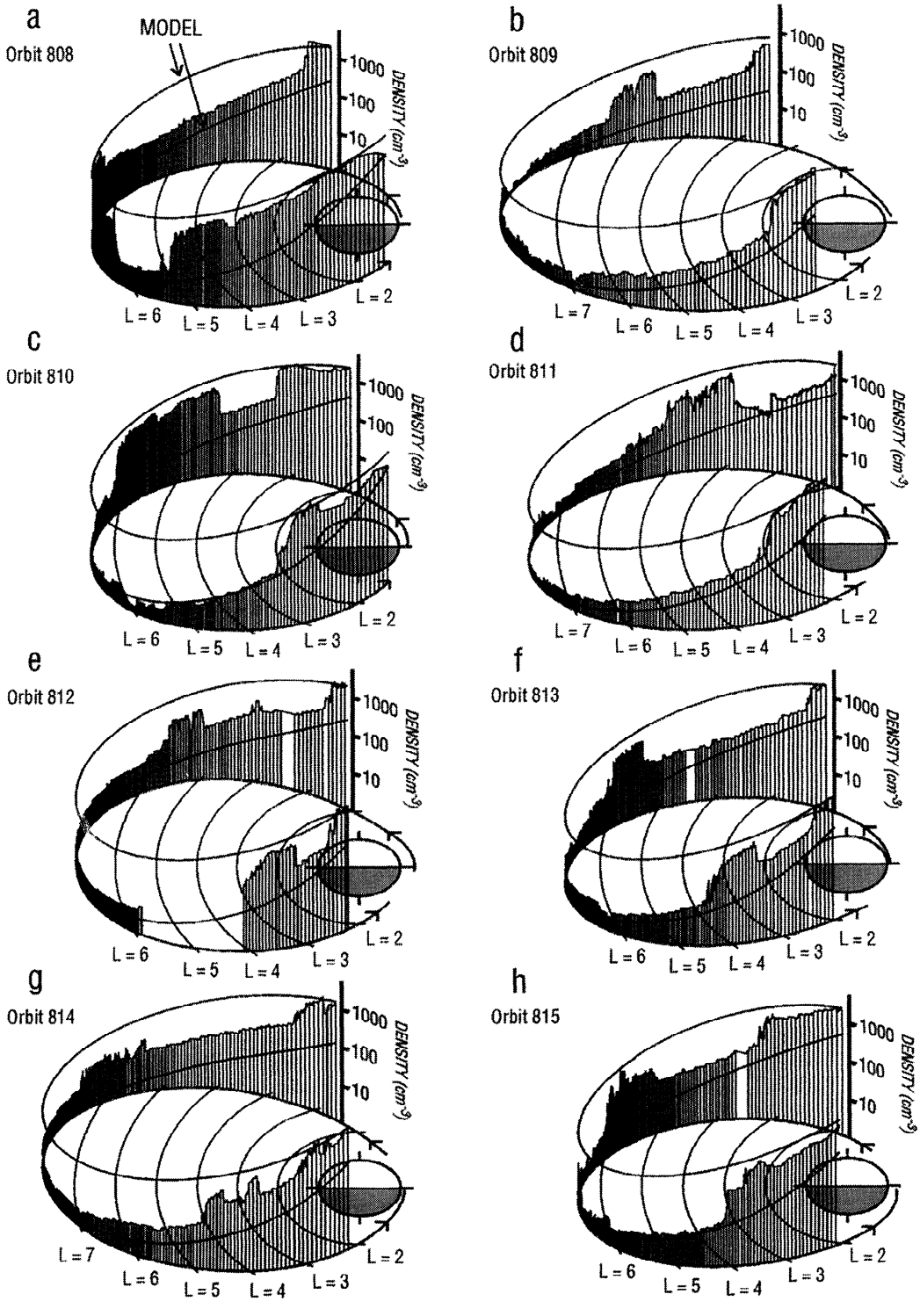

Figure 7. (a - h) Sequence of eight perspective plots for CRRES orbits 808 - 815 showing duskside density variations during a period of increased disturbance activity and subsequent quieting that extended from June 22 to June 26, 1991, as shown in Figure 8.

conditions during orbit 1033 are indicated in Figure 9a by fluctuations in the average value of the gyrofrequency f_H, especially in the 1430-1530 UT period. The pulsations along the gyrofrequency curve are an instrumental effect, produced by a beat between the 30 s CRRES spin period and an offset in the measured Z axis magnetic component. In Figure 9b the striations in the wave activity below the gyrofrequency are similarly instrumental, representing a beat between the satellite 30 s spin period and the 16 s data sampling interval.

Figure 10 provides a plot of the density along orbit 1033 from a perspective along the 2100 MLT meridian. Outbound in the prenoon sector (Figures 9a and 10) the satellite entered a trough-like region at $L \sim 2$. Then at $L \sim 2.2$ it encountered a narrow high-density feature bordering a broad low density region beyond. Near

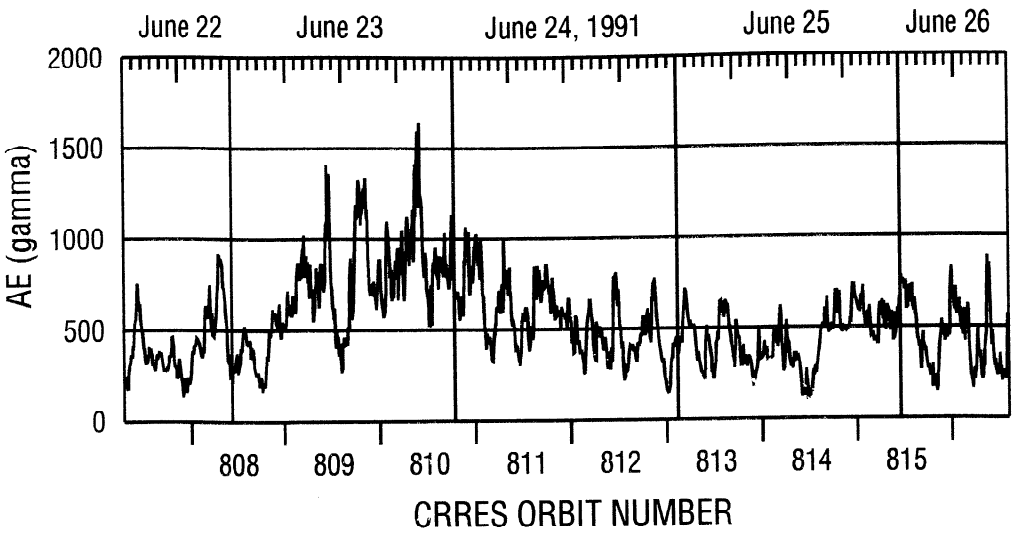

Figure 8. AE index for the period in Figure 7, where the CRRES orbital coverage is indicated below.

$L = 6$, at ~1130 UT (~1300 MLT), an extended, irregular patch of dense plasma was detected along a 10,000-km orbital segment, after which the density again dropped and varied irregularly. Later, at ~1530 UT (~1530 MLT) but still near L = 6, CRRES entered a region of plasmaspheric density. The region exhibited a number of narrow, deep fissures but otherwise extended relatively smoothly inward to $L \sim 3.7$, where an inner trough began as the density dropped by a factor of ~5 within a distance estimated to be less than 100 km. The density then varied smoothly at a level that was about a factor of 5 above the nighttime model curve for the main plasma trough. At L ~ 2.2 an inner plasmapause appears to have been crossed, but was only narrowly indicated owing to the 400-kHz upper limit of the SFR data.

2.2.4. Orbit 141: Troughs a low L values in the morning sector. An example of plasmaspheric cavities in the morning sector, similar in local time of occurrence to the case of Figure 5 but differing in many details, is shown in Figures 11-13. The geomagnetic conditions in this case, for orbit 141 on September 21, 1990, were less disturbed than in the cases from the dusk sector just noted, with *Kp* at 3 to 3+ following a brief increase to 5+ about 24 hours earlier. The full 10-hour record is shown in Figure 11, while details in the trough regions appear in Figures 12a and 12b and a perspective plot of density along the orbit is shown in Figure 13. On the outbound segment near 0030 MLT (see Figure 13) the density at first fell off relatively steadily until $L \sim 2.2$, at which point the slope increased sharply. Then at $L \sim 3.2$, after a further falloff within a trough-like region, the density rose abruptly by a factor of ~5 within less than 16 s along the CRRES orbit (16 s is twice the interval between successive SFR scans above 6.4 kHz). The outlier thus formed ended at $L \sim 3.5$ as the density dropped by a factor of ~30 into the main plasma trough region. No dense outliers were encountered near apogee as the density level remained close to the nighttime plasma trough model curve.

On the inbound segment near 0930 MLT (~0300 UT) a more gradual (compared to the night side) plasmapause was encountered at $L \sim 3.2$. Irregularities with spatial length ~300-400 km, an amplitude of ~ 50 el cm^{-3} and still finer small-scale structure, were observed throughout the region of plasmapause gradients (see Figure 12b). Near $L = 2.8$ the density dropped sharply by a factor of ~5 into an inner trough. A plasmapause-like density increase, more sharply defined than the change observed outbound near $L = 2.2$, also began at $L \sim 2.3$.

2.2.5. Orbit 290: A widespread depression in plasmaspheric density. Figures 14 and 15 show a different type of plasmaspheric density depression. Apogee in this case (orbit 290, November 21-22, 1990) was near 0300 MLT, and the perspective is from a point on the 2100 MLT meridian. Geomagnetic activity was only moderate; the *Kp* index had reached a maximum of ~4 in the preceding 24 hour period, and prior to that, values had been in the 2-4 range for several days. Outbound on the night side (Figure 15), density fell off gradually beyond $L \sim 2$, reaching a level similar to that found in the inner troughs by $L \sim 2.7$. It then remained at that level until about $L = 4.2$. Beyond $L \sim 4.2$ the density increased gradually to a peak near $L = 5$ and then fell off in plasmapause-like fashion to a relatively smooth main plasma trough. The inbound profile in the morning sector was similar to the nightside profile, except for slightly higher densities and displacement of the outlying peak to slightly larger L values. The symmetry of the data around apogee, as well as the small outbound/inbound differences, is consistent with approximate rotation of the plasma with the Earth (see section 2.4.4), accompanied by refilling fluxes from the ionosphere. This case appears to be one of a class in which (1) the density beyond some L value less than 3 is reduced by a factor of ~5 below quiet time levels and (2) an outlying higher-density feature, as that in Figure 14, may or may not be present and, if present, differs in form from typical outliers bordering inner troughs.

2.3. Waves Associated with Inner Troughs

2.3.1. Orbit 813. The wave emissions that appear on the SFR records offer insights into aspects of the density features, such as their roles as regions of wave generation and their longitudinal extent and variations. Such emissions can also provide information on the degree to which plasmaspheric cavities are "open" or "closed" in terms of access of waves to the region from outside or the ability of waves to escape from inside.

On orbit 813 (Figure 6a), two type-III solar bursts were detected in the main plasma trough region around apogee. In both cases they exhibited a lower cutoff at ~28 kHz, which is inferred to be the plasma frequency in the magnetosheath, below which solar bursts cannot penetrate into the magnetosphere. In contrast, plasma wave emissions above ~90 kHz appeared to be trapped in the trough at upper right, as they were in both troughs seen on orbit 146 in Figure 4. These emissions extended from the lowest UHR frequency

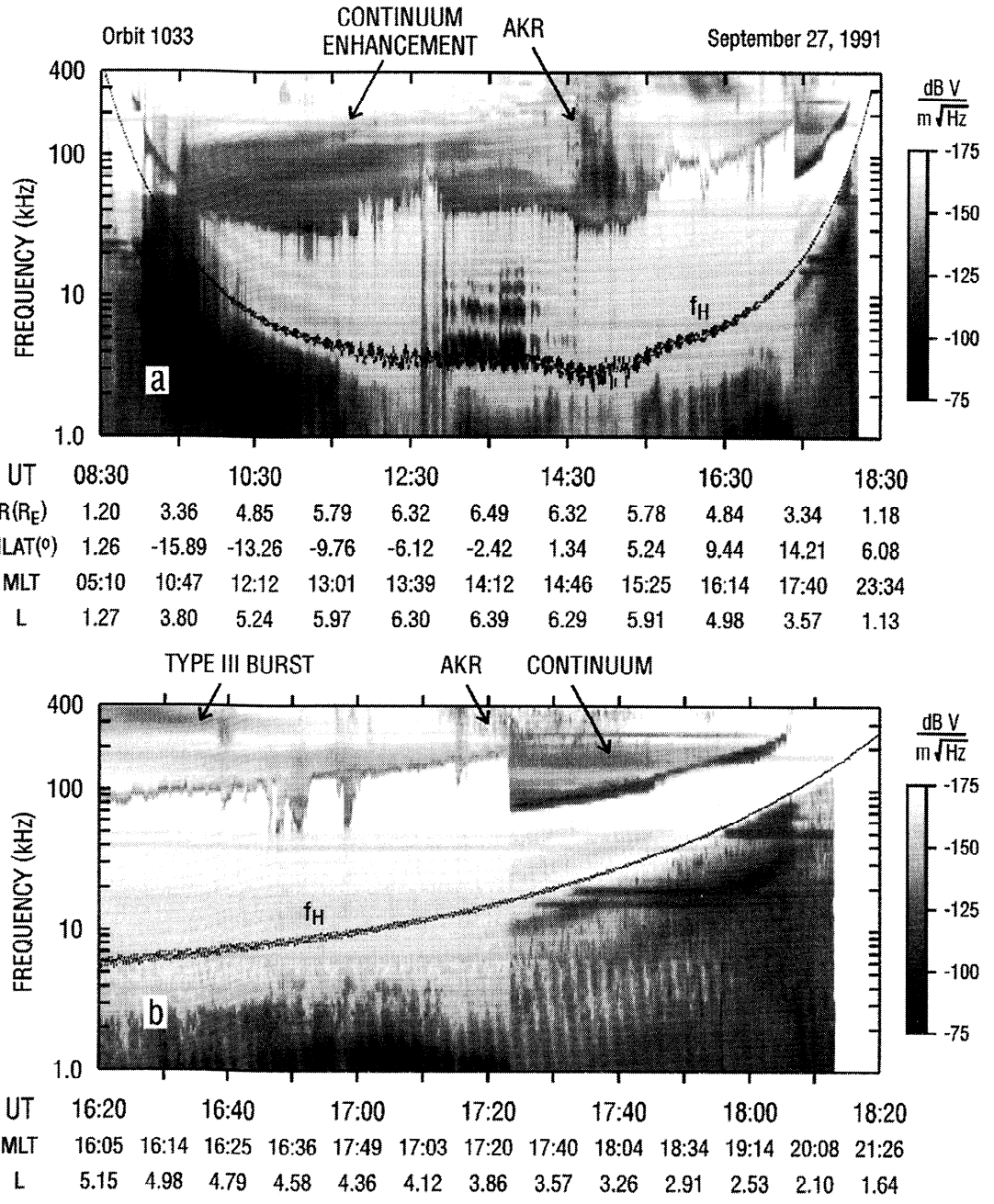

Figure 9. (a) SFR record from orbit 1033 on September 27, 1991, showing on the right evidence of a well-defined plasmaspheric cavity in the premidnight sector. (b) Expanded SFR record for the 2-hour period that included the inner trough at the right in Figure 9a.

representative of the outer wall to ~150 kHz, near the peak UHR frequency of the wall. This is presumably a high-frequency equivalent of the usual kind of continuum involving a wave mode that propagates back and forth between the inner and outer walls of the cavity, in a manner similar to the trapped continuum that is found to occur between the plasmapause and magnetopause [e. g., *Gurnett and Shaw*, 1973; *Kurth et al.*, 1981]. The plasmaspheric cavity in this case appeared to be at least partially closed, in much the same way that the main plasma trough or magnetospheric cavity is usually considered to be closed when trapped continuum is observed.

The emissions trapped in plasmaspheric cavities may be related to the so-called "kilometric continuum" recently reported by *Hashimoto et al.* [1999]. That radiation, which was detected by Geotail in the frequency range 100 - 800 kHz at an orbital distance of 10-30 R_E in the dayside and evening sectors of the magnetosphere, also appeared to be generated inside the plasmasphere.

During orbit 813 in Figure 6, AKR was regularly present, as might be expected from the ongoing substorm activity indicated in Figure 8. At the right, near 0700 UT, AKR was cut off in frequency above the high-density feature bordering the trough on the outside. We suggest that this cutoff was the result of wave refraction between the high-latitude source region of AKR, presumably at altitudes ranging from 2000 to 15,000 km [e.g., *Benson and Calvert*, 1979], and points along the CRRES orbit where the high-density feature was detected. The rays at frequencies close to the

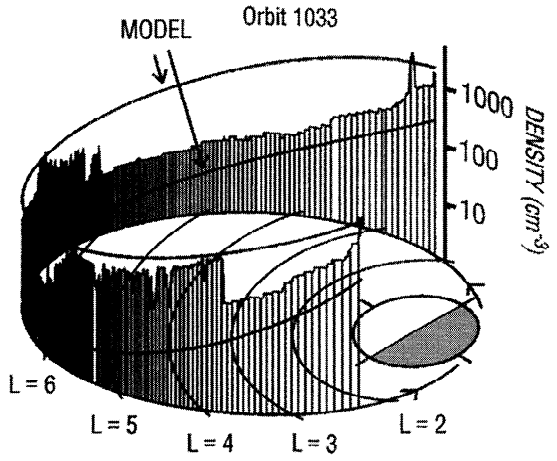

Figure 10. Perspective plot of the density data for orbit 1033 (Figure 9a), in this case from a viewpoint along the 2100 MLT meridian.

plasma frequency at points along the path between the source and CRRES would miss the spacecraft because of outward bending of the ray paths as they approached or slightly penetrated the high-density region just outside the trough, which we assume must have extended over at least 20° in longitude to have caused this effect (see section 2.4.5).

2.3.2. Orbit 1033. The SFR record of Figure 9a shows strong, diffuse bands of emissions that rose in frequency with time, the uppermost reaching ~200 kHz. The bands were strongest near local noon (see orbital track in Figure 10) but disappeared as the satellite approached 1500 MLT. This appears to be what is called a "continuum enhancement" by *Kasaba et al.* [1998], a surge of radiation, often rising in frequency, that is common during periods of substorm activity. The surge to frequencies well above the magnetosheath plasma frequency may represent an enhancement of the escaping continuum radiation that is generated at approximately the UHR frequency in the region of steep plasmapause density gradients in the late morning sector in the aftermath of substorm-associated plasmaspheric contraction. This would be consistent with the findings of *Gurnett* [1975] and of *Kurth et al.* [1981] that the source region of escaping continuum radiation is mostly in the morning sector and with the known tendency of the peak plasma frequency at the plasmapause to increase during a substorm. The time gap near 0920 UT between the UHR band at ~70-90 kHz and these emissions, as well as the disappearance of the rising emissions near 1430 UT, may be attributed to movement of the spacecraft into, and later out of, the radiation pattern of the emission source.

In the inner trough part of the SFR record (Figure 9b) there was once again continuum radiation extending up to and slightly above the upper frequency limit of the outer trough wall (the narrow band at ~250 kHz is believed to represent interference). The tendency for these trapped emissions to slightly exceed the upper frequency limit of the outer trough wall suggests that some of the emission frequency components originated at nearby longitudes where the outer wall of the trough rose to higher densities. The variation in emission amplitude with frequency appears to follow similar variations in the UHR frequency along the bottom of the trough. *Kurth et al.* [1981] inferred a causal connection between electrostatic UHR bands and bands of continuum radiation.

2.3.3. Orbit 141. In both inner troughs on orbit 141 (Figures 12a and 12b), continuum radiation above 100 kHz appeared to be trapped, much as in the case of orbit 813 in Figure 6. In the outbound trough near 0200 MLT these emissions extended slightly above the peak UHR frequency in the dense outer wall. On the other hand, in the inbound case near 1000 MLT in Figure 12b these emissions only reached an upper limit of ~230 kHz, significantly below the maximum UHR frequency of ~340 kHz at the inner edge of the outer trough wall. A descending type-III radio burst appeared to extend well below the peak UHR frequency of

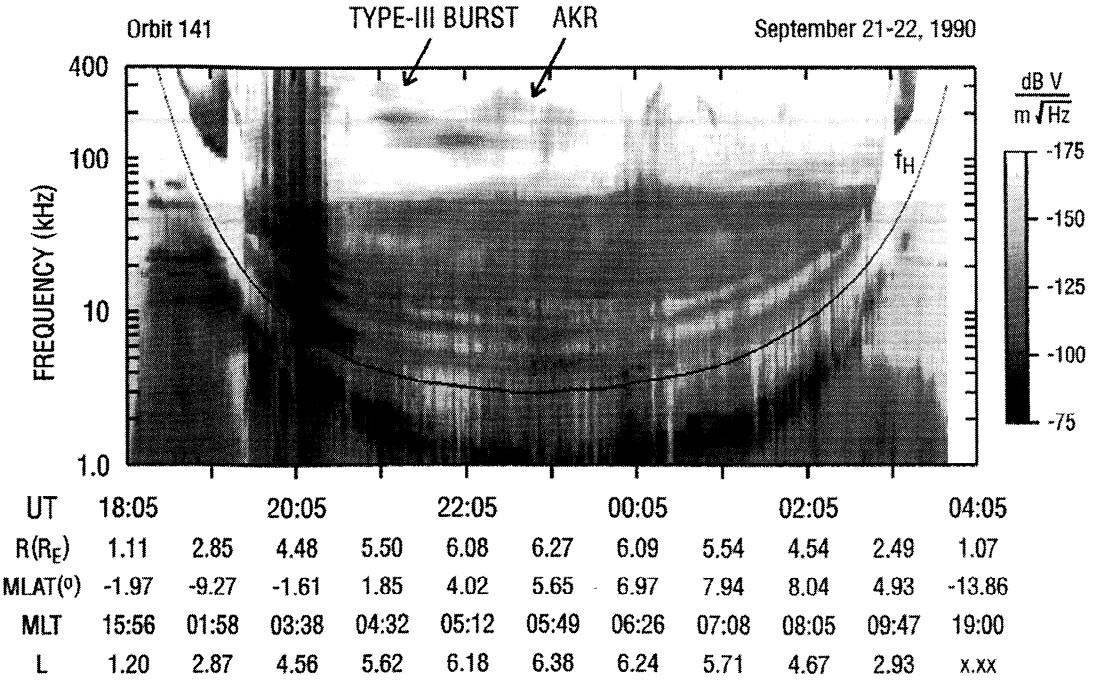

Figure 11. SFR record for orbit 141 on September 21, 1990, showing evidence of plasmaspheric cavities in the dawn sector.

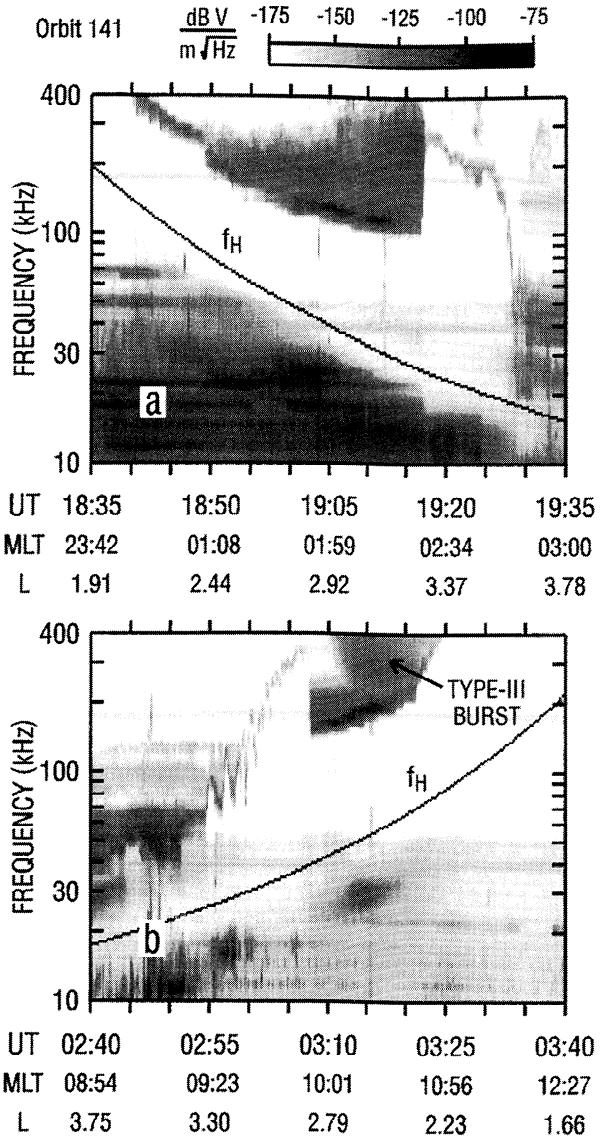

Figure 12. Expanded SFR records showing the inner troughs encountered during the (a) outbound and (b) inbound legs of orbit 141.

the outer wall, where it gradually merged with the pool of trapped continuum inside the trough. This suggests that the cavity was only partially closed, in that there was a way for continuum radiation generated in the cavity above ~230 kHz to escape and conversely a way for solar burst wave energy down to 230 kHz to enter the cavity and be detected by CRRES. We suggest that, as on orbit 1033, there was a density variation along the outer trough wall but in this case a region of reduced density at nearby longitudes.

2.4. Summary of Inner Trough Properties

2.4.1. Occurrence. All of the CRRES 10-hour SFR records like those illustrated in Figures 2 and 4 were surveyed for the occurrence of inner troughs. The criteria for a trough included a trough density at least a factor of 2 below nearby plasmaspheric levels and a trough width of $\Delta L \sim 0.3$ or more. Most such cases exhibited a steep outer density wall and wave emissions within the trough at frequencies above those of the trapped continuum in the main trough region. There were gaps in data coverage on some of the 1017 available SFR records. Altogether, there were 948 outbound cases with plasmaspheric coverage and 798 inbound cases. Inner troughs were found to occur on 134 or ~14% of the outbound passes and on 85 or ~11% of the inbound passes. There were therefore a total of 219 trough events on 1746 plasmasphere crossings, or ~13% of the total. This number is in reasonable agreement with the findings from DE 1 by *Horwitz et al.* [1990].

2.4.2. Density Profile. The inner boundaries of the plasmaspheric cavities were in all but a few cases at $L < 4$ and in over 60% of the cases at $L < 3$. In roughly half of the latter, or 66 cases, the inner boundary was found to be at $L < 2.5$. The trough inner boundaries tended to be plasmapause-like in form, with a density change by a factor of ~5 within $\Delta L < 0.3$. On occasion, irregularities appeared in this boundary region or beyond it in the trough itself. The outer trough boundary was usually in the range L = 3-4.5 and was steeper than the inner boundary, in some cases exhibiting a density jump by as much as a factor of ~5 within less than 100 km along the CRRES orbit.

Within the 18-hour interval from 1800 MLT to 1200 MLT, during which there were relatively few problems in trough identification, the wider troughs were found in the 1800-2400 MLT sector, with widths ranging from $\Delta L \sim 0.5$ to $\Delta L \sim 1.5$. In the few cases observed near dawn the widths were found to be of order $\Delta L = 0.5$. The data from orbit 1033 in Figure 10 illustrate this difference: a broad trough appeared in the early evening sector, and a narrow one, bordered by a very thin outlier, was crossed in the postdawn sector.

In several well-defined cases studied in detail the density within the trough varied smoothly at a level a factor of ~5 below nearby plasmasphere levels but a factor of ~2 - 5 above levels detected in the main plasma trough along the same orbit (see Figures 6b, 7e, 7f, 10, and 13). In general, in the interval between ~1800 and 1200 MLT, the density levels inside the troughs were lower than those in the nearby plasmasphere by factors ranging from ~2 to 5. In the afternoon sector, factor of ~10 density differences from plasmaspheric levels were found in some cases.

2.4.3. Occurrence in MLT. In the SFR survey, trough crossings were sorted according to the MLT when CRRES passed L = 3 either inbound or outbound. The histogram of Figure 16 shows that the percentage of orbits containing troughs was highest at nighttime, being 17% in the 1800-2400 MLT sector, 15% in the 0000-0600 MLT sector, 5% in the 0600-1200 MLT sector, and 12% in the 1200-1800 MLT sector. The percentage for 1200-1800 MLT is the least reliable, for reasons suggested in section 2.2.2 and discussed in section 3.2.3.

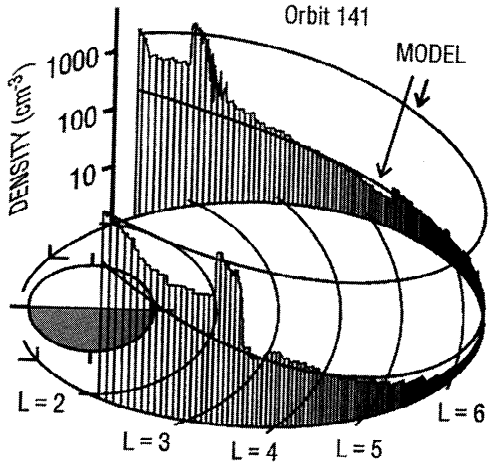

Figure 13. Perspective plot of the density data for orbit 141 (Figure 11), from a viewpoint along the midnight meridian.

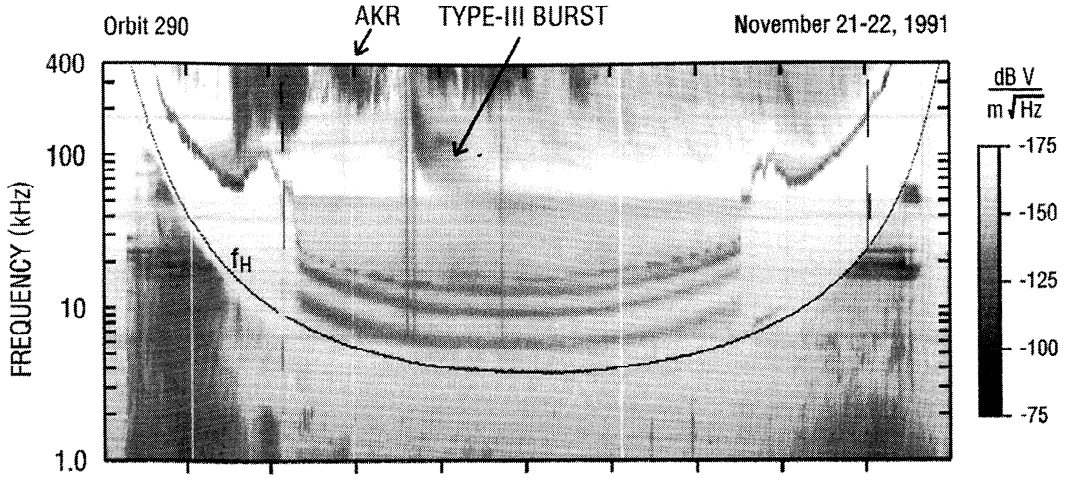

UT	22:40		00:40		02:40		04:40		06:40		08:40
R(R_E)	1.14	2.80	4.45	5.49	6.07	6.27	6.10	5.56	4.57	2.98	1.06
MLAT(°)	-14.86	18.69	20.27	20.84	21.29	21.52	21.33	20.32	17.57	9.36	-26.68
MLT	12:59	23:14	01:08	02:09	02:55	03:36	04:17	05:02	05:57	07:31	16:19
L	1.21	3.10	5.17	6.51	7.24	7.43	7.14	6.40	5.11	3.12	1.23

Figure 14. SFR record for orbit 290 on November 21-22, 1990, with apogee near 0300 MLT, illustrating a type of widespread density depression within the plasmasphere that appears to differ in form from the inner troughs shown in Figures 4 -13.

2.4.4. Duration. As illustrated in Figures 2 and 4, a deep trough could appear within 10 hours following a pass in which a trough was not evident in the same local time sector. Similarly, a deep trough could disappear between successive orbits. On the other hand, Figures 7e and 7f suggest that inner troughs in the post-dusk region could at times last for 10 hours or more.

To a rough approximation, CRRES was moving geosynchronously, since as illustrated in Figure 2, between $L \sim 3$ outbound and $L \sim 3$ inbound roughly 8 hours passed while the spacecraft advanced by ~ 6 hours in local time. A trough duration of ~8 hours or more is therefore suggested by Figures 5 and 13, because similar features occurred both outbound and inbound on the dawn side of the Earth during magnetically calm conditions. In these circumstances, approximate corotation of the plasma with the Earth might be expected. On the other hand, on the duskside and particularly during periods of moderate to strong geomagnetic activity, the tendency of the plasmasphere to corotate may be effectively suppressed beyond $L \sim 3$. Under such conditions, outbound and inbound features may differ substantially, as illustrated by essentially all of the cases in Figure 7.

2.4.5. Extent in Longitude. Several forms of evidence suggest that a well-defined inner trough can extend for at least 20° in longitude. This can be argued from the longitudinal extent of the inner trough segments shown in Figures 7e, 7f, and 10. It can also be argued in cases like those of Figures 5 and 13, in which CRRES appeared to detect the same trough outbound and then inbound. The satellite motion being only approximately geosynchronous, the trough crossings by CRRES must have been separated by ~ 20° in

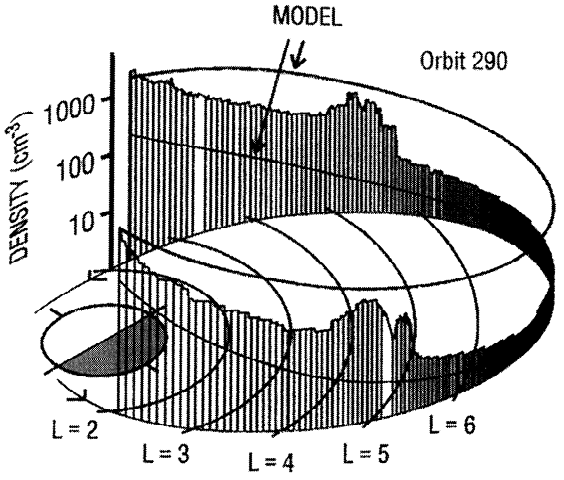

Figure 15. Perspective plot of the density data from orbit 290 (Figure 14) from a viewpoint along the 2100 MLT meridian.

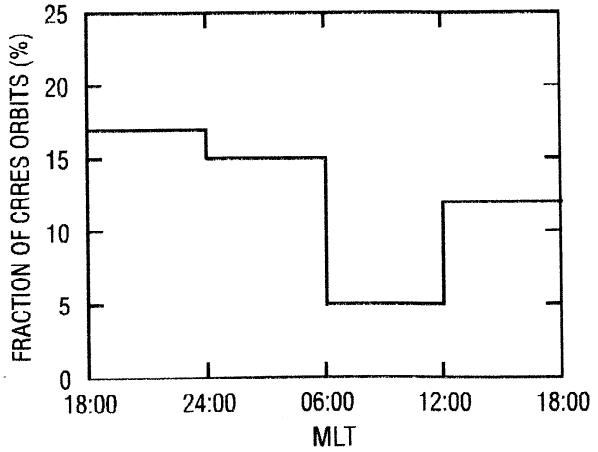

Figure 16. Histogram of the percentage of CRRES orbits within 6-hour MLT intervals during which inner troughs were detected by CRRES.

longitude if one assumes corotation of the trough structure with the Earth. Another argument can be based upon the efficient trapping of plasma wave emissions inside a trough, since repeated reflections at the trough walls are believed necessary for the development of trapped continuum [e.g., *Gurnett and Shaw,* 1973; *Kurth et al.,* 1981].

2.4.6. Extent along the Geomagnetic Field. We infer that the observed cavities extended along the field lines to the ionosphere, but we have not made confirming measurements, since the cases reported here were observed only within ~ 20° of the magnetic equator. We note, however, that the troughs reported in a statistical study by *Horwitz et al.* [1990] were made along high-inclination DE 1 orbits at a range of latitudes. We note further that the main plasmasphere, to which the inner troughs appear to be related in a vestigial sense, has been found to extend to ionospheric heights, for example, in whistler data on flux tube electron content [*Angerami and Carpenter,* 1966], in Alouette II observations of echoes from the plasmapause at ~1500-km altitude [*Clark et al.,* 1969], and also in the OGO 4 ion data of *Taylor et al.* [1971], which showed evidence that an inner trough extended down to an altitude of ~ 800 km.

2.4.7. Geomagnetic Conditions. As illustrated for orbits 812 and 813 in Figures 7 and 8, the observed inner troughs usually appeared in the aftermath of periods of enhanced geomagnetic activity. They were regularly found in CRRES records during and following periods in which the *Kp* index reached 5 or more.

3. Discussion

3.1. Real or Artificial Effects?

The reality of the troughs is supported by the fact that inner plasmaspheric regions of reduced density have now been found under similar geophysical circumstances from ground whistlers [*Carpenter,* 1970; *Ho and Carpenter,* 1976], from ion probes on OGO 4 [*Taylor et al.,* 1971] and DE 1 [*Horwitz et al.,* 1990], and from plasma wave instruments on EXOS D [*Oya,* 1991], ISEE 1 [*Carpenter et al.,* 1993], and CRRES.

The reality of the abrupt density change at the outer edge of a trough and of other details of the profiles is supported by the SFR plots themselves. Figures 9a and 9b show an abrupt change in whistler-mode wave intensity at the outer edge of a trough (~1723 UT). Activity below ~2 kHz was substantially stronger in the dense region outside the trough, while emissions between 4 and 10 kHz appeared to be trapped or enhanced within the trough. These abrupt changes can be attributed to guiding effects and wave reflection associated with an abrupt, geomagnetic-field-aligned boundary. For example, whistler-mode waves inside a trough that approach the boundary at relatively large wave normal angles (with respect to the magnetic field direction) would be expected to be refracted away from the dense outer region because of the rapid increase in refractive index at its inner edge. The waves would thus tend to be guided along the boundary in a whispering gallery mode as their wave normal angles oscillate around the off-axis Gendrin angle [*Gendrin,* 1961], at which the ray direction is along the magnetic field.

In the cases of Figures 6 and 12, plasma wave emissions largely filled low-*L* "biteouts" in the wave activity profiles. This implies that the bottom frequency in the biteouts can be interpreted as a local propagation cutoff at either the UHR or the plasma frequency and hence as a measure of local electron density. The UHR continued to appear on SFR records within the plasmasphere when density therein was a factor of ~5 below quiet time levels, as suggested by Figures 9a and 9b and also by Figure 14. In Figures 9a and 9b a band of wave emissions at the bottom of the trough appears comparable in width and definition to the UHR band in the dense region beyond, and in Figure 14 the UHR appears well defined everywhere interior to the main plasma trough even if the associated density levels near $L = 3$ are comparable to those at $L \sim 3$ inside inner troughs such as those in Figures 7e, 7f, and 10.

From a radio perspective, most inner troughs on the SFR records appeared to be plasmaspheric, in that there was a band of no activity below them extending down to the upper limit of whistler-mode wave activity at near one-half the local gyrofrequency. In the main plasma trough usually near apogee the spectrum below the lower limits of the pool of continuum radiation was regularly dominated by $n + ½$ ECH emissions [e.g., *Kennel et al.,* 1970; *Shaw and Gurnett,* 1975], as illustrated in Figures 6 and 11. Weak $n + ½$ ECH emissions also sometimes appear in an inner trough, as shown in Figure 9 near 1730 UT, where their upper cutoff in some cases was associated with the SFR bandwidth change at 50 kHz.

3.2. Interpreting the Density Profiles

3.2.1. Traditional paradigm. Can the development of inner troughs be explained in terms of the traditional paradigm involving the interplay of a large-scale convection electric field and the Earth's corotation field [e.g., *Nishida,* 1966; *Brice,* 1967; *Grebowsky,* 1970; *Chen and Wolf,* 1972]? According to this paradigm, a trough should develop at local times after dusk as the intensity of the convection electric field diminishes and a taillike, sunward extending dense plasma feature, a residual effect of plasmaspheric erosion, begins to rotate with the Earth. This implies that the inner and outer edges of the trough, as well as the outer edge of the dense region outside the trough, are translated vestigial boundaries of the taillike feature and main plasmasphere as those features existed prior to the onset of the quieting trend. Several features of the inner trough data are consistent with this scenario. As noted above, the troughs tended to appear in the aftermath of periods of enhanced geomagnetic activity. The finding that troughs in the premidnight sector were wider than those near dawn is also consistent with an inward spiraling model of taillike streamers [e.g., *Chen and Wolf,* 1972]. The density profiles at the inner limits of the troughs and the outer limits of the bordering outliers were plasmapause-like in structure, in that their scale widths (distance over which density drops by a fixed factor) and total density changes were consistent with findings from ISEE plasmapause crossings by *Carpenter and Anderson* [1992]. Those two boundary regions also contained embedded irregularities, as illustrated in Figures 4, 6b, and 12b. Such irregularities are known to be common in the plasmapause region [e.g., *Koons,* 1989; *Carpenter et al.,* 1993; *LeDocq et al.,* 1994; *Moldwin et al.,* 1995]. The density levels within the troughs were also consistent with this scenario, in that in the evening sector cases studied they tended to be comparable to or only slightly above those known to exist in the late afternoon main trough following dayside refilling from the ionosphere. This relationship can be seen in Figures 7e, 7f, and 10. At other times the inner trough levels tended to exceed the levels in the nearby main trough by factors of from ~2 to 5, in which cases the outer regions, as illustrated in Figures 4, 6b, 7f and 13, are inferred to have represented night-time main trough conditions. Statistically, these outer regions have been found to be a factor of ~5 below late afternoon main trough levels because of more limited exposure to refilling from the ionosphere [e.g., *Carpenter and Anderson,* 1992].

Inner trough plasma with a heritage of substantial dayside refilling might also be expected to be cooler than the main trough plasma observed by CRRES beyond the main plasmasphere, especially those with more limited earlier exposure to refilling or

greater exposure to the hot plasma of the plasma sheet. In their study of embedded trough effects appearing in 0 to 50-eV ion data from DE 1, *Horwitz et al.* [1990, p. 7947] found the associated plasma to be in all cases "typical cold isotropic plasmaspheric plasma, albeit at lower densities than the surrounding regions." That the plasmas in the inner trough regions were indeed cooler than those beyond the main plasmasphere is also suggested by the absence of strong n + ½ ECH bands during trough crossings, as indicated in Figures 4, 6, and 11. Such bands are considered indicative of warm plasma conditions [e.g., *Kennel et al.,* 1970; *Shaw and Gurnett,* 1975].

Several features of the inner troughs are not easily accommodated by the simple quieting model. They include (1) the inward extension of a significant number of troughs to $L < 2.5$; (2) the steepness of the trough outer walls; (3) the apparent detachment from the main plasmasphere of the dense plasmas bordering some inner troughs, and (4) the occasional occurrence of complex density structure within inner troughs or in their vicinity.

3.2.2. Occurrence of a plasmapause at $L < 2.5$. Judging by the boundaries of the inner troughs illustrated in Figures 7e, 7f, 10, and 13, and the fact that ~30% of the inner troughs identified in the CRRES data had boundaries at $L < 2.5$, it seems clear that the plasmasphere radius may be reduced, at least locally, to the vicinity of $L = 2$ under geophysical conditions for which statistical studies [e.g. *Carpenter,* 1967; *Carpenter and Anderson,* 1992] would predict radii in the range $L = 3$ - 3.5 (preceding *Kp* index in the range 5 to 6+). Furthermore, the data suggest that in such cases a plasmapause could exist at $L \sim 2.2$ over a wide longitude range. In Figures 7e and 7f, for example, if one compares the inbound data from orbit 812 with the outbound data from 813, recorded only 1.5 hours later but 9 hours earlier in MLT, it can be argued that during much of the time of the two orbits a plasmapause existed at L ~ 2.2 on an essentially global basis.

There is much scatter in the data on which the predictions of plasmapause locations are based. Most of those data are from $L > 3$ for reasons having to do with spatial limits on available whistler and ISEE coverage [e.g., *Carpenter,* 1967; *Carpenter and Anderson,* 1992]. It is possible that erosion to the depths implied by these measurements happens more readily near solar maximum, when CRRES was operating, rather than in the quiet sun years reflected in the whistler (1963) and ISEE (mostly 1982-1983) data.

Drift meter data from multiple DMSP satellites show that near dusk, fast, narrowly channeled westward subauroral ion drift events (SAIDs) are at times embedded in broader regions of westward plasma flow that extend well inside $L = 3$ (P. Anderson, personal communication, 1999). Furthermore, CRRES double-probe electric field data from magnetic storm periods have been found to show larger potential differences between $L = 2$ and 4 than between $L = 4$ and 6 [*Wygant et al.,* 1998; *Burke et al.,* 1998]. These concentrations of storm time electric fields at low L values, in possible conjunction with the narrower SAID flows, might help to explain some of the complexities of dusk-sector plasmas, including the particular effects noted in sections 2.2.2 and 2.2.3.

3.2.3. Steepness of the outer wall and the question of connectivity. Is the dense outlier bordering the inner trough essentially detached from the main plasmasphere or is it connected to that body in some other local time sector? In their case study of light ion ionospheric trough effects at $L \sim 2$ - 3, *Taylor et al.* [1971] made a persuasive case for the existence of a connected tail-like feature. In addition, in a series of case studies involving multiple satellites and ground whistlers, *Carpenter et al.* [1993, p. 19,268] found that "the properties of outliers observed near the plasmapause and out to synchronous orbit suggest that many of these are rooted in or attached to the main body of the plasmasphere." However, the authors also found that "the distribution and occurrence of dense plasmas observed at L ~ 6 and beyond . . . suggest that many of those regions are effectively isolated from or detached from the main plasmasphere."

It is tempting to suggest that in a case in the dusk sector such as orbit 813 in Figure 7f, the two outliers detected, one before and one after 1800 MLT, were simply cuts through a single tail-like cold plasma feature that was more or less fixed in sun-Earth coordinates for ~10 hours and was connected to the main plasmasphere somewhere on the night side. However, if we believe that the plasmapause was at $L \sim 2.2$ at all longitudes during much of the time of the two orbits, as suggested above, such a connection becomes difficult to visualize.

It is possible that in cases such as this the outlier bordering the inner trough had previously been detached from a larger plasmasphere because of localized structure in the convection electric field, as might occur during subauroral ion drift events [e.g., *Galperin et al.,* 1974; *Anderson et al.,* 1991; *Ober et al.,* 1997], or as a consequence of instabilities in the plasmapause region [e.g., *Lemaire,* 1974, 1975; *Kelley,* 1986; *Carpenter et al.,* 1993]. Its steep inner edge might then reflect the physical processes involved in the detachment.

It might also be argued that the steepness of the inner wall is a natural consequence of the movement of a preexisting plasmapause boundary along converging flow streamlines. Although some drift paths during quieting periods might indeed have a steepening effect on an existing profile, if an inner trough is simply a mapped version of the boundaries of the afternoon plasmasphere, and of a feature extending sunward therefrom, its outer wall would presumably have a scale width (in which 90% or more of the density change has occurred) that is more characteristic of the afternoon dayside plasmapause, that is, of 1000 km or more, and we would not expect predominantly corotational motion during quieting to reduce that scale width to near or less than the 100-km values that have been observed.

It is noteworthy that the density profiles in Figures 7f and 10 were similar inside $L \sim 3$ but different in the regions beyond $L = 3$. Qualitatively, this might be regarded as evidence of domination by the Earth's corotation electric field inside $L \sim 2.5$ in comparison to its influence in the region beyond, where the effects of temporally varying and spatially structured convection electric fields as well as instabilities may have been relatively more important. The persistent influence of the convection field at the higher L shells is suggested not only by the similarity of the outlying density structures on orbits 812 and 813 but also by the fact that in the afternoon (outbound) sector on those orbits (and on orbit 1033) the ratio of the density in the main plasma trough to the model values for night-time (lower model curve) increased with increasing L. Such density increases could be the result of increases with L in flux-tube residence times, and hence in cumulative density replenishment from the ionosphere associated with increases with L in the influence of the convection electric field.

3.2.4. Relationship of inner troughs to widespread density depressions. It is not clear how the inner troughs are related to widespread density depressions such as the one illustrated in Figure 15. Some such depressions, especially those unaccompanied by outlying regions of higher density, may reflect deep and persistent penetration of the plasmasphere by convection electric fields, such that outliers do not remain near the eroded plasmasphere to form inner troughs. The outlying density increases that are observed in such cases may develop when a radial profile with certain form undergoes the effects of flux tube compression during cross-L flow [e.g., *Park and Carpenter,* 1970]. On the other hand, some of the widespread depressions may be pronounced versions of the

localized density depressions, by factors of as much as ~3, that have been found from whistler measurements inside the eroded plasmasphere in the aftermath of periods of enhanced convection [e.g., *Park and Carpenter,* 1970]. Case studies suggested that within the longitude sectors affected, this phenomenon involves dumping into the ionosphere of an amount of plasma comparable to the amount lost through erosive cross-L motions at higher L values [e.g., *Park,* 1973; *Carpenter and Lemaire,* 1997]. The mechanism of dumping is not yet well understood. *Park* [1971, 1973] proposed that it involves the effects of cross-L inward convection on the distribution of O+ in the ionospheric O+ to H+ charge exchange region where the low-altitude boundary conditions on plasmaspheric H+ are determined.

4. Concluding Remarks

Trough-like density depressions in the plasmasphere equatorial density profile were found in early whistler work [*Carpenter,* 1970; *Ho and Carpenter,* 1976]. In satellite studies, density troughs in the plasmasphere in the L = 2-3 range were reported from OGO 4 by *Taylor et al.* [1971], from DE 1 by *Horwitz et al.* [1990], and from EXOS D by *Oya* [1991]. Such inner troughs, which we consider to be manifestations of geomagnetic-field-aligned density cavities, were found during 13% of the 1746 plasmasphere crossings documented in the CRRES sweep frequency receiver (SFR) data in 1990-1991. In these observations the plasmapause-like inner boundaries of the troughs were usually at $L < 3.5$, and in roughly 30% of the cases they were at $L < 2.5$ under geophysical conditions that have traditionally been associated with plasmapause radii at larger L values, in the L = 3 - 3.5 range.

The troughs, found at all local times, were most common in the 1800-2400 MLT sector, in general agreement with *Horwitz et al.* [1990], and least common between 0600 and 1200 MLT. Density levels in several well-defined troughs were found to be a factor of ~5 below nearby plasmasphere levels. Variations in the depression factor between ~2 and 10 in the overall data set probably account for the various stages of density recovery. Trough widths in L varied from $\Delta L \sim 0.5$ to $\Delta L \sim 1.5$, where those in the premidnight sector tended to be wider than those detected near dawn. The gradients at the outer trough boundaries tended to be particularly steep, where in one case the density jumped by a factor of ~5 within < 100 km along the satellite orbit, as abruptly as in any observed plasmapause crossing thus far reported.

As delineated on SFR records by the upper hybrid resonance emission band, inner troughs often contain a pool of radiation that is similar to trapped continuum but at a higher frequency. The apparent trapping of this radiation, as well as the shielding of auroral kilometric radiation from inside the troughs, suggests that the associated plasmaspheric cavities extend in longitude over a range of at least 20°, and probably more. Such a longitudinal extent is also suggested by the length of CRRES orbital segments within troughs.

On some CRRES orbits the plasmaspheric density was found to be reduced by a factor of ~5 from quiet-time plasmaspheric levels over wide ranges in L value beginning near L = 2. In such cases a steep outer boundary of the depressed region was not observed, although an outer density peak was sometimes present. Such depressions may be the result of deeply penetrating convection electric fields that are more persistent than those associated with the inner troughs. Another possibility is that they are primarily due to plasma losses to the ionosphere, as opposed to the motions transverse to B that are probably involved in the inner trough effects.

We suggest that the inner trough effects are essentially a quieting phenomenon, appearing as translated vestiges of plasma configurations established during preceding periods of plasmaspheric erosion. In some cases the outlying plasmas involved may be extensions of the main plasmasphere. However, in the case of troughs with steep outer walls the preceding plasma configurations may have involved a mechanism for detaching plasma from an originally larger main plasmasphere, such as by the shear flows associated with subauroral ion drifts (SAIDs). In the case of troughs with inner boundaries at $L < 2.5$ the subauroral convection electric field must have achieved comparable inward penetration. Such penetration is likely to have occurred near dusk, as suggested by recent reports from DMSP drift meter studies and from double-probe electric field measurements on CRRES.

Much can be learned about plasmaspheric cavities from existing data sets, for example, about their occurrence, about the extent of correlated ionospheric effects, and about correlated changes in particle and wave activity. Key questions about the origin and global extent of the cavities can hopefully be answered during imaging missions in which photon and radio techniques are used to remotely investigate the plasmasphere [*Williams et al.,* 1992; *Frank et al.,* 1994; *Calvert et al.,* 1995; *Green et al.,* 1998].

Acknowledgments. We are indebted to Connie Cheung of Stanford University for help in development of the method of displaying electron density measurements along CRRES orbits and to Dave Lauben of Stanford for advice on the method. We are also grateful to Joseph Lemaire and Leonardo Fedullo of IASB in Brussels for assistance with an earlier implementation of the method. Work at Florida Institute of Technology was supported by NASA grants NAGW-5153 and NAG5-4897.

Janet G. Luhmann thanks Dennis Gallagher and another referee for their assistance in evaluating this paper.

References

Anderson, P. C., R. A. Heelis, and W. B. Hanson, The ionospheric signatures of rapid subauroral ion drifts, *J. Geophys. Res., 96,* 5785, 1991.

Anderson, R. R., D. A. Gurnett, and D. L. Odem, CRRES plasma wave experiment, *J. Spacecr. Rockets, 29* (4), 570, 1992.

Angerami, J. J., and D. L. Carpenter, Whistler studies of the plasmapause in the magnetosphere, 2, Equatorial density and total tube electron content near the knee in magnetospheric ionization, *J. Geophys. Res., 71,* 711, 1966.

Ashour-Abdalla, M., C. F. Kennel, and W. Livesey, A parametric study of electron multiharmonic instabilities in the magnetosphere, *J. Geophys. Res., 84,* 6540, 1979.

Benson, R. F., and W. Calvert, ISIS-1 observations at the source of auroral kilometric radiation, *Geophys. Res. Lett., 6,* 479, 1979.

Burke, W. J., N. C. Maynard, M. P. Hagan, R. A. Wolf, G. R. Wilson, L. C. Gentile, M. S. Gussenhoven, C. Y. Huang, T. W. Garner, and F. J. Rich, Electrodynamics of the inner magnetosphere observed in the dusk sector by CRRES and DMSP during the magnetic storm of June 4-6, 1991, *J. Geophys. Res., 103,* 29,399, 1998.

Brice, N. M., Bulk motion of the magnetosphere, *J. Geophys. Res., 72,* 5193, 1967.

Calvert, W., et al., The feasibility of radio sounding in the magnetosphere, *Radio Sci., 30,* 1577, 1995.

Carpenter, D. L., Relations between the dawn minimum in the equatorial radius of the plasmapause and *Dst, Kp* and local *K* at Byrd Station, *J. Geophys. Res., 72,* 2969, 1967.

Carpenter, D. L., Whistler evidence of the dynamic behavior of the duskside bulge in the plasmasphere, *J. Geophys. Res., 75,* 3837, 1970.

Carpenter, D. L., and R. R. Anderson, An ISEE/whistler model of equatorial electron density in the magnetosphere, *J. Geophys. Res., 97,* 1097, 1992.

Carpenter, D. L., and J. Lemaire, Erosion and recovery of the plasmasphere in the plasmapause region, *Space Sci. Rev., 80,* 153, 1997.

Carpenter, D. L., C. G. Park, H. A. Taylor Jr., and H. C. Brinton, Multi-experiment detection of the plasmapause from Eogo satellites and Antarctic ground stations, *J. Geophys. Res., 74,* 1837, 1969.

Carpenter, D. L., B. L. Giles, C. R. Chappell, P. M. E. Decreau, R. R. Anderson, A. M. Persoon, A. J. Smith, Y. Corcuff, and P. Canu, Plasmasphere dynamics in the duskside bulge region: a new look at an old topic, *J. Geophys. Res., 98,* 19,243, 1993.

Chappell, C. R., Detached plasma regions in the magnetosphere, *J. Geophys. Res., 79,* 1861, 1974.

Chappell, C. R., K. K. Harris, and G. W. Sharp, The dayside of the plasmasphere, *J. Geophys. Res., 76,* 7632, 1971.

Chen, A. J., and R. A. Wolf, Effects on the plasmasphere of a time-varying convection electric field, *Planet. Space Sci., 20,* 483, 1972.

Clark, W. L., Jr., J. R. McAfee, R. B. Norton, and J. M. Warnock, Radio wave reflections from large horizontal gradients in the topside ionosphere, *Proc. IEEE, 57* (4), 493, 1969.

Elphic, R. C., L. A. Weiss, M. F. Thomsen, and D. J. McComas, Evolution of plasmaspheric ions at geosynchronous orbit during times of high geomagnetic activity, *Geophys. Res. Lett., 23,* 2189, 1996.

Frank, L. A., et al., Imagers for the magnetosphere, aurora, and plasmasphere, *Opti. Eng., 33* (2), 391, 1994.

Gallagher, D. L., P. D. Craven, R. H. Comfort, and T. E. Moore, On the azimuthal variation of core plasma in the equatorial magnetosphere, *J. Geophys. Res., 100,* 23,597, 1995.

Galperin, Y. I., V. L. Khalipov, and A. G. Zosimova, Plasma convection in the polar ionosphere, *Ann. Geophys., 30,* 1, 1974.

Gendrin, R., Le guidage des whistlers par le champ magnetique, *Planet Space Sci., 5,* 274, 1961.

Grebowsky, J. M., Model study of plasmapause motion, *J. Geophys. Res., 75,* 4329, 1970.

Grebowsky, J. M., N. K. Rahman, and H. A. Taylor Jr., Comparison of Ogo 3 and Ogo 4 hydrogen ion composition measurements, *Planet Space Sci., 18,* 965, 1970.

Green, J. L., W. W. L. Taylor, S. F. Fung, R. F. Benson, W. Calvert, B. W. Reinisch, D. L. Gallagher, and P. H. Reiff, Radio remote sensing of magnetospheric plasmas, in *Measurement Techniques in Space Plasma: Fields, Geophys. Monogr. Ser.*, vol. 103, edited by R. F. Pfaff, J. E. Borovsky, and T. D. Young, p. 193, AGU, Washington, D. C., 1998.

Gurnett, D. A., The Earth as a radio source: The nonthermal continuum , *J. Geophys. Res., 80,* 2751, 1975.

Gurnett, D. A., and R.R. Shaw. Electromagnetic radiation trapped in the magnetosphere above the plasma frequency, *J. Geophys. Res., 78,* 8136, 1973.

Gurnett, D. A., R. R. Anderson, F. L. Scarf, R. W. Fredricks, and E. J. Smith, Initial results from the ISEE-1 and -2 plasma wave investigation. *Space Sci. Rev., 23,* 103, 1979.

Hashimoto, K., W. Calvert, and H. Matsumoto, Kilometric continuum detected by Geotail, *J. Geophys. Res., 104,* 28,645, 1999.

Higel, B., and L. Wu, Electron density and plasmapause characteristics at 6.6 R_E: A statistical study of the GEOS 2 relaxation sounder data, *J. Geophys. Res., 89,* 1583, 1984.

Ho, D., and D. L. Carpenter, Outlying plasmasphere structure detected by whistlers, *Planet. Space Sci., 24,* 987, 1976.

Horwitz, J. L., R. H. Comfort, and C. R. Chappell, A statistical characterization of plasmasphere density structure and boundary locations, *J. Geophys. Res., 95,* 7937, 1990.

Hubbard, R. F., and T. J. Birmingham, Electrostatic emissions between electron gyroharmonics in the outer magnetosphere, *J. Geophys. Res., 83,* 4837, 1978.

Kasaba, Y., H. Matsumoto, K. Hashimoto, R. R. Anderson, J.-L. Bougeret, M. L. Kaiser, X. Y. Wu, and I. Nagano, Remote sensing of the plasmapause during Geotail observation of nonthermal continuum enhancement, *J. Geophys. Res., 103,* 20389, 1998.

Kelley, M. C., Intense sheared flow as the origin of large-scale undulations of the edge of the diffuse aurora, *J. Geophys. Res., 91,* 3225, 1986.

Kennel, C. F., F. L. Scarf, R. W. Fredricks, J. H. McGehee, and F. V. Coroniti, VLF electric-field observations in the magnetosphere, *J. Geophys. Res., 75,* 6136, 1970.

Koons, H. C., Observations of larger-amplitude, whistler mode wave ducts in the outer plasmasphere, *J. Geophys. Res., 94,* 15,383, 1989.

Kurth, W. S., D. A. Gurnett, and R. R. Anderson, Escaping nonthermal continuum radiation, *J. Geophys. Res., 86,* 5519, 1981.

LeDocq, M. J., D. A. Gurnett, and R. R. Anderson, Electron number density fluctuations near the plasmapause observed by CRRES spacecraft, *J. Geophys. Res., 99,* 23,661, 1994.

Lemaire, J., The 'Roche-limit' of ionospheric plasma and the formation of the plasmapause, *Planet. Space Sci., 22,* 757, 1974.

Lemaire, J., The mechanisms of formation of the plasmapause, *Ann. Geophys., 31,* 175, 1975.

Lemaire, J., and K. I. Gringauz, *The Earth's Plasmasphere*, Cambridge Univ. Press, New York, 1998.

Mayr, H. G., J. M. Grebowsky, and H. A. Taylor Jr., Study of the thermal plasma on closed field lines outside the plasmasphere, *Planet. Space Sci., 18,* 1123, 1970.

McComas, D. J., S. J. Bame, B. L. Barraclough, J. R. Donart, R. C. Elphic, J. T. Gosling, M. B. Moldwin, K. R. Moore, and M. F. Thomsen, Magnetospheric plasma analyzer (MPA): Initial three-spacecraft observations from geosynchronous orbit, *J. Geophys. Res., 98,* 13,453, 1993.

Moldwin, M. B., Outer plasmaspheric plasma properties:What we know from satellite data, *Space Sci. Rev., 80,* 181, 1997.

Moldwin, M. B., M. G. Thomsen, S. J. Bame, D. J. McComas, and K. R. Moore, An examination of the structure and dynamics of the outer plasmasphere using multiple geosynchronous satellites, *J. Geophys. Res., 99,* 11,475, 1994.

Moldwin, M. B., M. F. Thomsen, S. J. Bame, D. McComas, and G. D. Reeves, The fine-scale structure of the outer plasmasphere, *J. Geophys. Res., 100,* 9649, 1995.

Nishida, A., Formation of plasmapause, or magnetospheric plasma knee, by the combined action of magnetospheric convection and plasma escape from the tail, *J. Geophys. Res., 71,* 5669, 1966.

Ober, D. M., J. L. Horwitz, and D. L. Gallagher, Formation of density troughs embedded in the outer plasmasphere by subauroral ion drift (SAID) events, *J. Geophys. Res., 102,* 14,595, 1997.

Oya, H., Studies on plasma and plasma waves in the plasmasphere and auroral particle acceleration region, by PWS on board the EXOS-D (Akebono) satellite, *J. Geomagn. Geoelectr., 43,* 369, 1991.

Paranicas, C., W. J. Hughes, H. J. Singer, and R. R. Anderson, Banded electrostatic emissions observed by the CRRES plasma wave experiment, *J. Geophys. Res., 97,* 13,889, 1992.

Park, C. G., Westward electric fields as the cause of night-time enhancements in electron concentrations in the midlatitude *F* region, *J. Geophys. Res., 76,* 4560, 1971.

Park, C. G., Whistler observations of the depletion of the plasmasphere during a magnetospheric substorm, *J. Geophys. Res., 78,* 672, 1973.

Park, C. G., and D. L. Carpenter, Whistler evidence of large-scale electron-density irregularities in the plasmasphere, *J. Geophys. Res., 75,* 3825, 1970.

Shaw, R. R., and D. A. Gurnett, Electrostatic noise bands associated with the electron gyrofrequency and plasma frequency in the outer magnetosphere, *J. Geophys Res., 80,* 4259, 1975.

Taylor, H. A., Jr., H. C. Brinton, D. L. Carpenter, F. M. Bonner, and R. L. Heyborne, Ion depletion in the high-latitude exosphere: Simultaneous OGO 2 observations of the light ion trough and the VLF cutoff, *J. Geophys. Res., 74,* 3517, 1969.

Taylor, H. A. Jr., J. M. Grebowsky, and W. J. Walsh, Structured variations of the plasmapause: Evidence of a corotating plasma tail, *J. Geophys. Res., 76,* 6806, 1971.

Weiss, L. A., R. L. Lambour, R. C. Elphic, and M. F. Thomsen, Study of plasmaspheric evolution using geosynchronous observations and global modeling, *Geophys. Res. Lett., 24,* 599, 1997.

Williams, D. J., E. C. Roelof, and D. G. Mitchell, Global magnetospheric imaging, *Rev. Geophys., 30* (3), 83, 1992.

Wygant, J., D. Rowland, H. J. Singer, M. Temerin, F. Mozer, and M. K. Hudson, Experimental evidence on the role of the large spatial scale electric field in creating the ring current, *J. Geophys. Res., 103,* 29,527, 1998.

R. R. Anderson, Department of Physics and Astronomy, 203 Van Allen Hall, University of Iowa, Iowa City, 52242. (email: rra@space.physics.uiowa.edu).

W. Calvert, 219 Friendship Street, Iowa City, IA 52245. (email: wcx@home.com).

D. L. Carpenter, Star Laboratory, Electrical Engineering Department, Stanford University, Stanford, CA 94305. (email: dlc@nova.stanford.edu).

M. B. Moldwin, Department of Physics and Space Science, Florida Institute of Technology, Melbourne, 32901. (email: moldwin@galileo.pss.fit.edu).

(Received January 12, 2000; revised April 4, 2000;
accepted April 24, 2000.)